# MONTHLY WEATHER REVIEW

VOLUME 78 NUMBER 5

MAY 1950

CONTENTS



U. S. DEPARTMENT OF COMMERCE · WEATHER BUREAU

## NOTICE OF CHANGE IN MONTHLY WEATHER REVIEW

The monthly climatological data tables carried in the MONTHLY WEATHER REVIEW through December 1949 now appear in "Climatological Data, National Summary". The subscription price to "Climatological Data, National Summary" is 15 cents per copy or $1.50 per year; remittance (payable to Treasurer of the United States) and correspondence regarding subscriptions should be sent to Superintendent of Documents, Government Printing Office, Washington 25, D. C.

DEPARTMENT OF COMMERCE
CHARLES SAWYER, Secretary

WEATHER BUREAU
F. W. REICHELDERFER, Chief

# MONTHLY WEATHER REVIEW

Editor, JAMES E. CASKEY, Jr.

Volume 78
Number 5

MAY 1950

Closed July 5, 1950
Issued August 15, 1950

## FORECASTING RADIATION FOG AT ELKINS, W. VA.

ROBERT A. HOOVER

Weather Bureau Airport Station, Washington, D. C.

[Manuscript received December 1, 1948; revised March 1950]

### ABSTRACT

Charts based on variables selected from data available on the preceding evening are developed for forecasting radiation fog at Elkins, W. Va., for autumn and winter months. The variables found useful in forecasting this fog include gradient wind velocity, surface temperature, and dew point depression. One of the interesting findings is that on relatively clear nights easterly gradient winds are more favorable for the formation of radiation fog than are westerly gradient winds. This and other physical aspects of the formation of the fog are discussed.

### INTRODUCTION

#### PROBLEM

One of the problems which occurs almost daily in forecasting for Elkins, W. Va. is that of determining whether or not radiation fog will form during the following night. Elkins is situated in the Tygart River Valley in the Allegheny Mountains with most of the higher ridges to the east of the station (fig. 1). The river flows in a south to north direction just west of the station and considerably higher ground immediately surrounds the station on all other sides. Since it is so protected from the wind, rapid cooling occurs after sunset on relatively clear nights and in many cases this process leads to the formation of fog. This investigation was undertaken in an effort to develop aids in forecasting this phenomenon largely through a quantitative test and analysis of some of the forecasting principles and rules already in use by forecasters. These rules emphasize the importance of variations of gradient wind speed and direction. In the course of the investigation additional factors were introduced in order that a more complete forecasting system could be developed for use subsequent to the determination of the information yielded by the gradient wind. These variables were then combined statistically into a set of charts by means of a graphical correlation procedure.


FIGURE 1.—Topographical map of the Elkins, W. Va., area.

893180—50——1

### DATA

The month of August was initially selected for study since it is the month with the greatest frequency of radiation fog at Elkins (see table 1). August data for the years 1942 through 1949 were analyzed with those for 1943 and 1949 being withheld for testing purposes. Data for nights during which the sky was cloudy (high overcast, or low broken or overcast) or precipitation occurred, or during which there was a frontal passage were not included in the study. The weather elements used were gradient wind direction and speed, as approximated from the 1930 EST surface map by means of a geostrophic wind scale applied to the sea-level isobars, and temperature and dew point at sunset as interpolated from the hourly observations. Data were tabulated from the hourly observations as to whether the visibility lowered to less than one mile in fog as well as the earliest time this occurred.

TABLE 1.—*Percentage of nights visibility at Elkins lowers to less than 1 mile due to radiation fog.*

| Month | Number of years | Percentage of relatively clear nights | Percentage of all nights |
|---|---|---|---|
| July | 2 | 50 | 26 |
| August | 5 | 76 | 38 |
| September | 4 | 59 | 32 |
| November | 5 | 18 | 7 |
| December | 5 | 14 | 4 |
| January | 6 | 29 | 6 |
| February | 3 | 10 | 2 |

## THE FORECASTING CHARTS

### CONSTRUCTION

As the first step in the development of the forecasting procedure the cases on which the study is based were plotted on a polar graph. This showed immediately that the material could be readily stratified into two parts since the cases with gradient winds from north through south via west showed a much lower percentage frequency of fog* cases than those with gradient winds from north-northeast through south-southeast via east. A third group was made up of cases when a ridge of high pressure was centered over Elkins and gradient wind was not measurable. Within these first two groups the gradient wind speed and difference between the temperature and dew point at sunset were examined for their joint effect on the reduction of visibility to less than one mile in radiation fog the following night as well as on the earliest time this occurred (cf. [1], [2]).

Figure 2 with these independent variables as coordinates was constructed for westerly gradient winds by the following procedure. If fog reduced the visibility to less than 1 mile, the time was entered corresponding to that particular gradient wind speed and dew point depression. If the visibility was not reduced to less than 1 mile during the night, "N" was entered on the chart. For the construction of frequency and time isopleths the data were arbitrarily divided into small groups of about five readings per group. This arbitrary division is shown in figure 2 by the light solid lines. The percentage frequency and time of occurrence were then found for each group and placed on the charts near the location that would seem to best represent the average location of the readings. Time and frequency isopleths were then drawn for these values and are shown in figure 2 as dark solid lines.

Since Taylor [1] presumably found that temperature was also a variable to be considered in the construction of fog prediction diagrams, figure 3, with this as a variable together with the difference between the temperature and

*The word "fog" henceforth in this paper means visibility restricted to less than 1 mile in radiation fog.

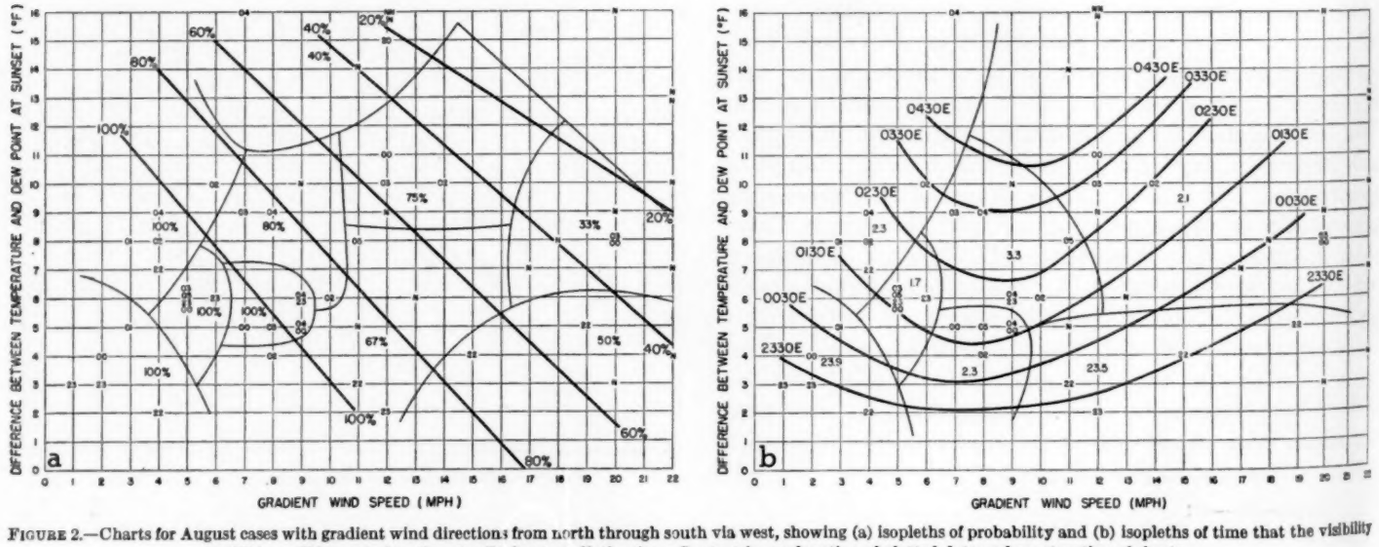


FIGURE 2.—Charts for August cases with gradient wind directions from north through south via west, showing (a) isopleths of probability and (b) isopleths of time that the visibility at Elkins will lower to less than 1 mile due to radiation fog. See text for explanation of plotted data and construction of charts.

dew point at sunset was constructed. The time isopleths were drawn by using the same method of groupings as was done in figure 2b.

Now in order that the relationship suggested by figure 2b could be combined with the relationship suggested by figure 3, figure 4 was constructed using a technique suggested by Brier [3]. The times of occurrences for all the cases with westerly gradient winds were estimated. For each case there were two estimated times of formation, one from figure 2b and one from figure 3. Then with these sets of readings as coordinates, the corresponding actual time of formation was plotted on figure 4 and the time isopleths drawn. However, it was found that the linear correlation coefficient relating predictions obtainable from the latter chart was no higher than could be obtained from figures 2b and 3 taken separately. This result was found also for the charts for easterly gradient cases.

A similarly constructed set of charts with the same variables as those used in figures 2–4 was prepared for cases with easterly gradient winds. These diagrams are shown in figures 5–7.

Figure 8 is made up from cases when a ridge of high pressure was centered over Elkins and no gradient wind was measurable. These cases showed 100 percent chance of occurrence, so this figure merely suggests a time of occurrence.

Charts for September and winter months (November through February) were made following the same procedure as that used for August. The winter months were grouped together because there seemed to be little advantage to be gained from the use of the individual charts for each month; in fact the advantage of having more data to use in the preparation of the charts probably made them more accurate as the percentage of nights with fog was much lower than for August and September. No work was done on the month of October. Only the charts for August are shown in this paper but the others are similar in appearance to those for August.

## TESTS

After noting that figures 4 and 7 added little to the correlations, a test was made of figures 2, 5, and 8 for August 1943 and 1949, comparing their forecasts with the official airway forecasts on clear nights when no clouds were fore-

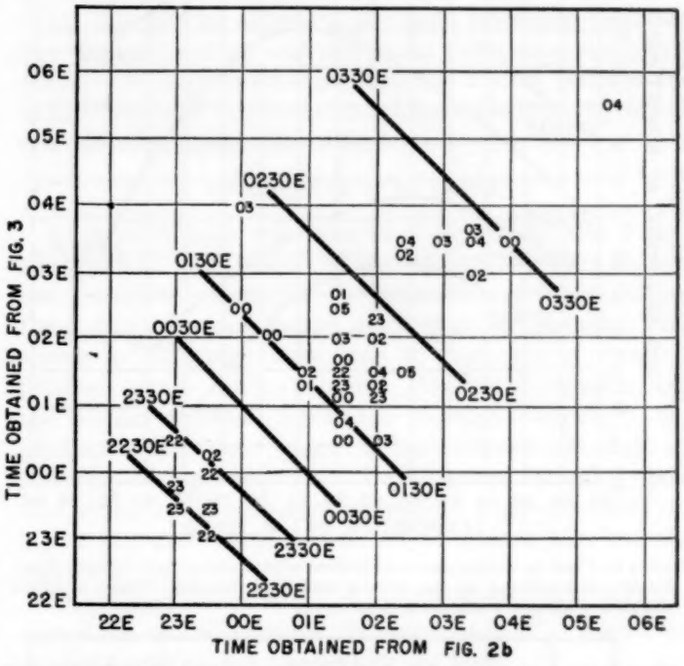


FIGURE 4.—Chart for August cases with gradient wind directions from north through south via west, showing isopleths of time that visibility at Elkins will lower to less than 1 mile due to radiation fog. Time in this chart is given as a function of the times from figures 2b and 3.

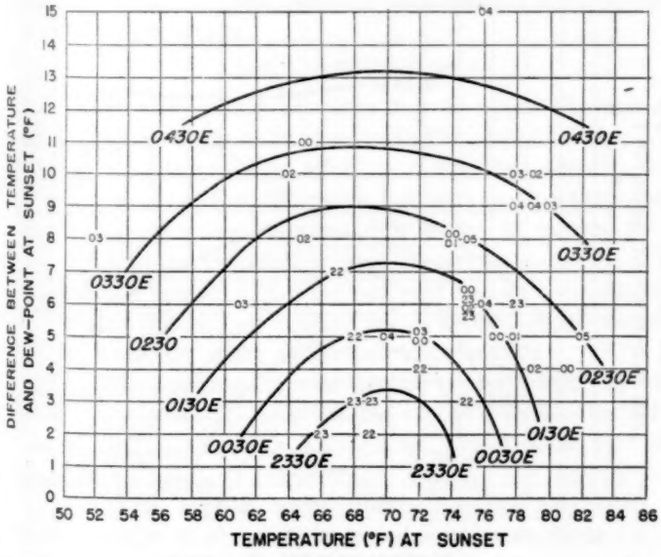


FIGURE 3.—Chart for August cases with gradient wind directions from north through south via west, showing isopleths of time that visibility at Elkins will lower to less than 1 mile due to radiation fog.

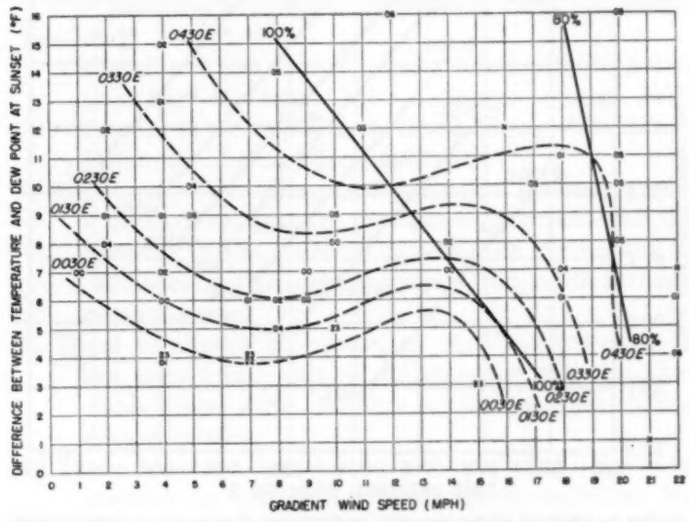


FIGURE 5.—Chart for August cases with gradient wind directions from north-northeast through south-southeast via east, showing isopleths of probability (solid lines) and time (dashed lines) that visibility at Elkins will lower to less than 1 mile due to radiation fog.

cast in the official airway forecast. The results of this test are tabulated in table 2. A separate tabulation was made for each month since the charts were consulted each evening in August 1949 before the official forecast was made. The average error per forecast with regard to time of formation came out to be 1.8 hours for official airway forecast and 1.2 hours for the charts.

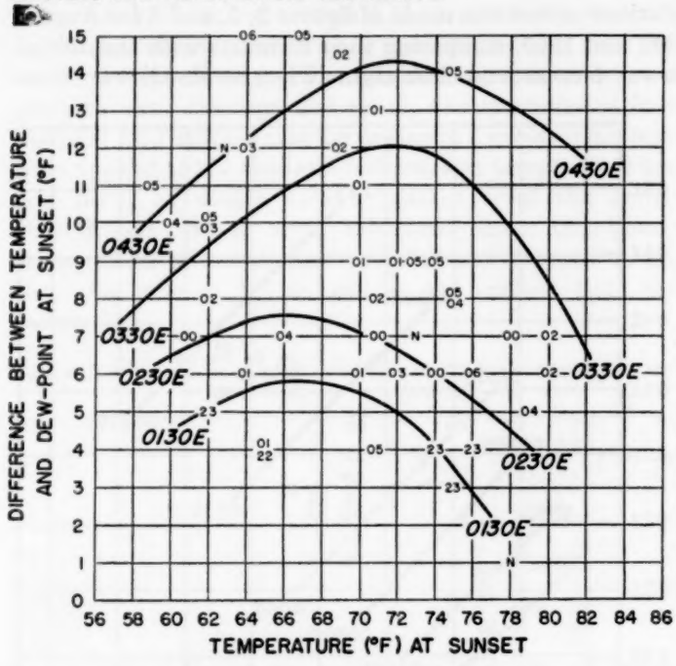


FIGURE 6.—Chart for August cases with gradient wind directions from north-northeast through south-southeast via east, showing isopleths of time that visibility at Elkins will lower to less than 1 mile due to radiation fog.

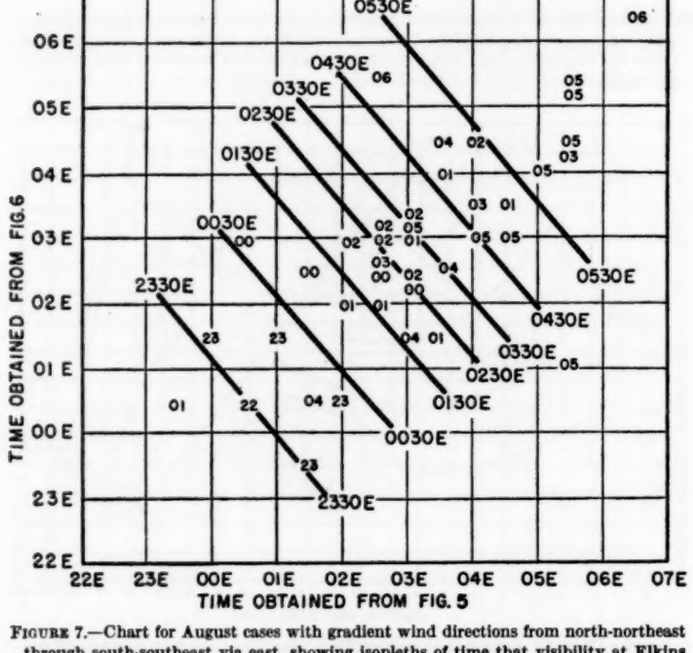


FIGURE 7.—Chart for August cases with gradient wind directions from north-northeast through south-southeast via east, showing isopleths of time that visibility at Elkins will lower to less than 1 mile due to radiation fog. Time in this chart is given as a function of the times from figures 5 and 6.

TABLE 2.—*Contingency tables comparing official airway forecasts and forecasts from the charts for 1948 and 1949*

| OBSERVED | OFFICIAL AIRWAY FORECAST | | | FORECAST FROM THE CHARTS | | |
|---|---|---|---|---|---|---|
| | 1943 | | | 1943 | | |
| | Fog | No fog | Totals | Fog | No fog | Totals |
| Fog | 13 | 4 | 17 | 17 | 0 | 17 |
| No fog | 1 | 0 | 1 | 1 | 0 | 1 |
| Totals | 14 | 4 | 18 | 18 | 0 | 18 |
| | 1949 | | | 1949 | | |
| Fog | 11 | 3 | 14 | 14 | 0 | 14 |
| No fog | 3 | 1 | 4 | 3 | 1 | 4 |
| Totals | 14 | 4 | 18 | 17 | 1 | 18 |
| | 1943 and 1949 | | | 1943 and 1949 | | |
| Fog | 24 | 7 | 31 | 31 | 0 | 31 |
| No fog | 4 | 1 | 5 | 4 | 1 | 5 |
| Totals | 28 | 8 | 36 | 35 | 1 | 36 |

EXAMPLES

The following two examples outline the use of these charts. Let us start with the following readings—gradient wind velocity west 10 m. p. h. (determined from 1930 EST surface map), temperature at sunset 70° F., dew point depression at sunset 10° F. Figure 2 gives about 65 percent chance of occurrence and a time of formation of about 0400 EST. Now going to Figure 3 we get a time of formation of about 0300 EST. Using these two readings for time on figure 4, we get a final time of occurrence of 0330 EST. For another example consider gradient wind southeast 10 m. p. h., temperature 80° F., dew point depression 12° F. Figure 5 yields 100 percent chance and a time of 0500 EST. Figure 6 suggests a time of 0430 EST. Using these two readings for time on figure 7, we get a final time of occurrence of 0530 EST.

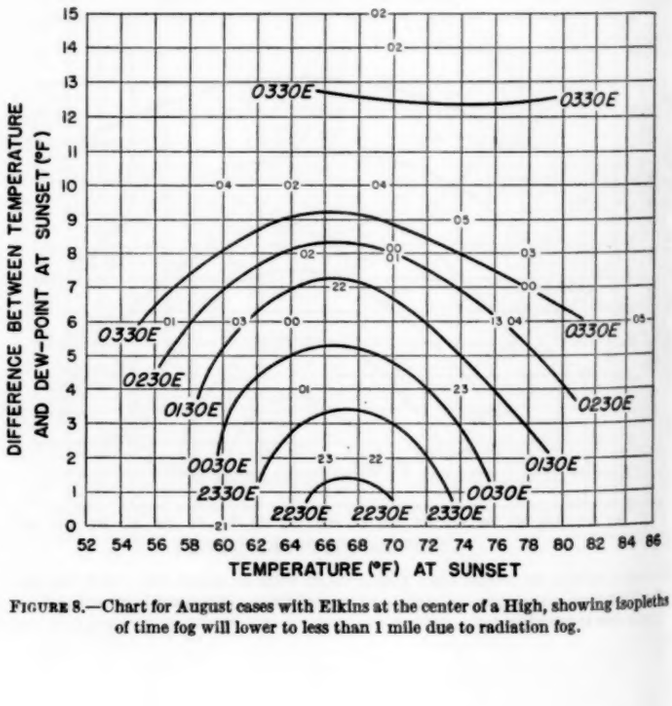


FIGURE 8.—Chart for August cases with Elkins at the center of a High, showing isopleths of time fog will lower to less than 1 mile due to radiation fog.

## PHYSICAL ASPECTS OF FOG FORMATION

### EFFECTS OF LOCAL TOPOGRAPHY

In the course of developing the forecasting procedure, several physical aspects of fog formation were investigated. An investigation to find a reason for the greater predominance of radiation fog with an easterly flow as compared to a westerly flow was made. The data showed that sunset dew points averaged slightly lower for the easterly cases and the average difference between the temperature and the dew point at sunset was larger for the easterly cases; neither of these findings could be used to explain the greater predominance of radiation fog associated with the easterly gradient winds. It is possible that in the case of Elkins, the greater frequency of fog cases with an easterly flow is due to the fact that Elkins is more sheltered from the wind when it is blowing from an easterly direction than when it is blowing from a westerly direction (fig. 1). Greater cooling of the air near the ground will occur in the former case because there will be less mixing of the air than in the latter case. This point may be examined further by considering figure 9. As shown in the sketch, station "A", located similarly to Elkins relative to the ridge, is situated so that it would be more protected from an easterly wind than station "B" would be. In this case the fall in temperature, due to nocturnal radiation, would be greater at station "A" than at station "B" since at station "B" the easterly surface wind would tend to disturb the air near the surface. In both cases there would be possibility of drainage of cool air down the side of the mountain but since the coolest air would be at the lower points, most of the air coming down the sides of the mountain would flow above the cooler air at the bottom. It is also possible that the relationship lies principally in the greater stability of the air masses present with easterly as compared with westerly winds.

### EFFECT OF TEMPERATURE

Figures 3, 6, and 8 all show fog to occur the earliest when temperatures at sunset are in the upper sixties. To further investigate this effect a chart (not shown) was plotted showing the difference between temperature and dew point at sunset against dew point at sunset using data for August, September, and the winter months. The greatest percentages of occurrence of fog and the earliest times of formation were found for dew-point temperatures at sunset in the upper fifties and lower sixties.

The probable mechanism of the phenomenon as suggested by Mook [2] in a similar analysis of Taylor's fog predicting diagram for Kew [1] is briefly this: For the same dew point depression at sunset, fog occurs less frequently at higher temperatures because according to Brunt [4], the higher moisture values are associated with a decrease in net outgoing radiation; and at lower temperatures, according to Petterssen [5], the air lacks sufficient moisture to produce fog. Therefore, at some middle point, there will be a maximum frequency of fog. However, as might be expected, the most favorable combination of temperature and dew-point depression is slightly different at the two stations, Kew and Elkins, perhaps due to differences in the coefficient of heat conductivity of the soil and other geographical factors.

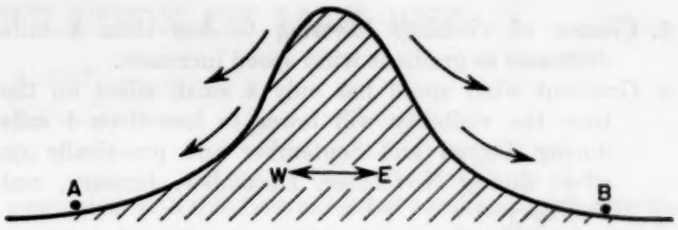


FIGURE 9.—Sketch showing effect of a mountain on nocturnal cooling in valleys on either side.

### OTHER ASPECTS OF THE CHARTS

It appears from examination of figures 2b and 5 that the gradient wind speed (within the range of data shown) has less effect on the time of formation of fog at Elkins than does the dew-point depression at sunset. This seems to be particularly true in the case of westerly gradient winds during August. During September and the winter months (November through February), the gradient wind speed seems to have almost no effect on the time of fog formation. Both figures 2a and 5 show that in general the greater the gradient wind speed and the larger the dew point depression at sunset, the less the chance of fog.

One aspect which is not readily explainable is that the time lines on both figures 2b and 5 have dips where the gradient winds are 5 to 10 miles per hour.

## CONCLUSIONS

The following conclusions are drawn from this investigation:

1. Visibilities of less than 1 mile at Elkins due to radiation fog are much more common during July, August, and September than during November, December, January, and February.
2. Gradient winds from north-northeast through south-southeast via east are much more favorable for the lowering of the visibility to less than 1 mile due to radiation fog than gradient winds from north through south via west.
3. There is almost no chance of visibility lowering to less than 1 mile due to radiation fog with gradient winds from north through south via west during winter months.
4. There is better than an even chance of the visibility lowering to less than 1 mile due to radiation fog during August and September with gradient winds from north-northeast through south-southeast via east.

5. Chance of visibility lowering to less than 1 mile decreases as gradient wind speed increases.
6. Gradient wind speed has only a small effect on the time the visibility will lower to less than 1 mile during August and September and practically no effect during November, December, January, and February.
7. The smaller the depression of the dew point at sunset, the greater the chance the visibility will lower to less than 1 mile due to radiation fog and the earlier it will occur.
8. During the winter months the lower the temperature at sunset, the less likely the visibility will lower to less than 1 mile due to radiation fog and the earlier it will form. Also it is not likely to form if the temperature at sunset is less than 30° F.
9. When radiation fog at Elkins becomes deep enough to produce a "ceiling", this "ceiling" will be zero more than 90 percent of the time.

## ACKNOWLEDGMENTS

I wish to express my thanks to Mr. Conrad Mook for his many suggestions regarding the preparation of the charts and to Mr. Samuel Pearce for his aid in collection of the data. Thanks are also due to the many other members of the forecasting staff at Washington National Airport who have contributed ideas during the course of this study.

## REFERENCES

1. G. I. Taylor, "The Formation of Fog and Mist," *Quarterly Journal of the Royal Meteorological Society*, vol. 43, No. 183, July 1917, pp. 241–268.
2. Conrad P. Mook, "Some Remarks Concerning Taylor's Fog Prediction Diagram," *Bulletin of the American Meteorological Society*, vol. 31, No. 6, June 1950, pp. 206–209.
3. G. W. Brier, "A Study of Quantitative Precipitation Forecasting in the TVA Basin," U. S. Weather Bureau *Research Paper No. 26*, November 1946.
4. D. Brunt, "Notes on Radiation in the Atmosphere I," *Quarterly Journal of the Royal Meteorological Soceity*, vol. 58, No. 247, October 1932, pp. 389–418.
5. S. Petterssen, "Some Aspects of Formation and Dissipation of Fog," *Geofysiske Publikasjoner*, vol. 12, No. 10, June 1939, pp. 5–22.

# THE WEATHER AND CIRCULATION OF MAY 1950[1]

EUGENE J. AUBERT

Extended Forecast Section, U. S. Weather Bureau

Washington, D. C.

The outstanding feature of the average circulation over North America and the adjacent oceans for May 1950 was the abnormal northeastward displacement of the east Pacific High and its extension as a ridge into western Canada (see fig. 1). A trough with below-normal heights extended from south central Canada through the southwestern United States, while a ridge with above-normal heights covered the east coast of the United States. The Low in northeast Canada was displaced southwest of its normal location for May, as shown by the field of 700-mb. height departures from normal. Although the trough associated with this Low extended southeastward, into the western Atlantic, the minimum in the 700-mb. height anomaly field extended south-southwestward, connecting with the negative height anomalies in the Dakotas. This resulted in stronger-than-normal northwesterly flow into the region centered in Montana and Wyoming while the general area from Texas to Michigan experienced a stronger-than-normal southwesterly flow.

The westerlies in the eastern Pacific were located about 10° north of normal and were very well developed. This is indicated in figure 1 by the strong gradient of the 700-mb. height anomaly to the south of the Gulf of Alaska and was

[1] See Charts I-XI, following page 89, for analyzed climatological data for the month.

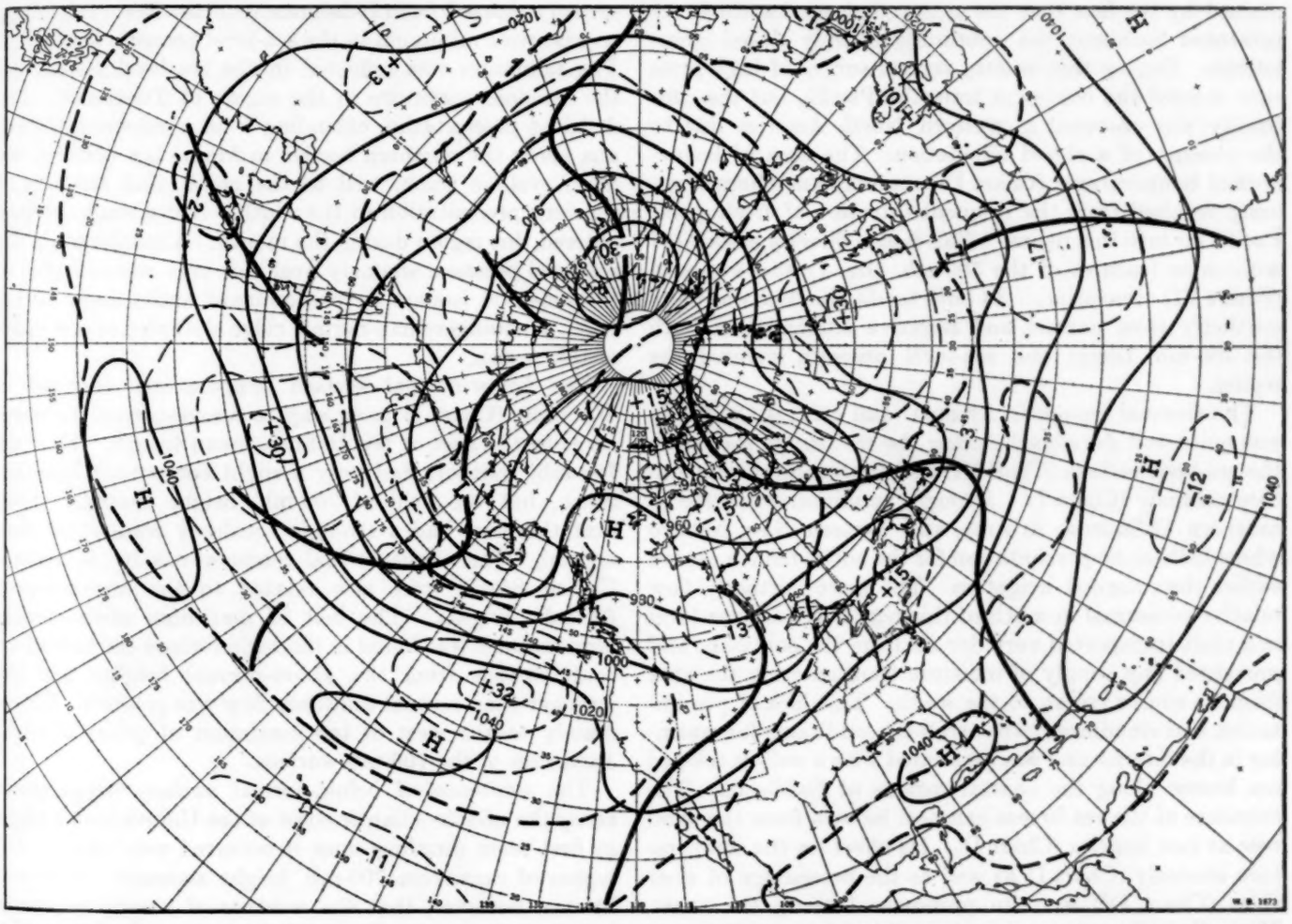


FIGURE 1.—Mean 700-mb. chart for the 30-day period May 2-31, 1950. Contours at 200-foot intervals are shown by solid lines, 700-mb. height departures from normal at 100-foot intervals by dashed lines, with the zero isopleth heavier. Anomaly centers and contours are labeled in tens of feet. Minimum latitude trough locations are shown by heavy solid lines.

associated with the more northerly location of the east Pacific anticyclone. These circulation features had a pronounced effect on the track of cyclones in this region, as shown in Chart III. The west coast of the United States was mainly lacking in cyclonic activity entering from the Pacific, an abnormal circumstance for the month of May. The cyclone tracks were shifted northward into Canada, the storms moving eastward generally along the mean flow at the 700-mb. level and a well defined east-west trough of mean sea-level pressure. The anomaly of precipitation (Chart V insert) is a vivid portrayal of the lack of cyclones in the western United States, where a considerable deficiency of precipitation was observed. It is interesting to note that the anticyclone tracks (Chart II) show only one polar Pacific High entering North America, especially since the average conditions along and off the west coast were so predominantly anticyclonic with a nose of high pressure and positive anomaly protruding into the state of Washington at sea level. This can be explained by the fact that the anticyclone tracks which are presented represent the continuity of only closed circulations. During this month, several surges of high pressure entered the continent from the Pacific, but the continuity was obscured in western North America due to the absence of a closed circulation. The area of below-normal temperatures (Chart I) centered in northern Wyoming resulted from the frequent intrusion of fresh polar Pacific air into this region. This is also directly associated with some features of the 700-mb. (fig. 1) and sea-level (Chart VI) circulation. At both levels, the flow was more northerly than normal, and negative anomalies of both the 700-mb. height and sea-level pressure covered the region.

The thermal trough in Arizona and central California was quite well developed during the month, as shown by the sea-level isobars (Chart VI) and the sea-level temperature anomaly (Chart I). Drought conditions occurred in southern California, Arizona, and western New Mexico where little or no precipitation for the entire month caused earlier than normal irrigation. The more northerly flow relative to normal in much of this region at both sea level and aloft transported very dry air from the continent and prevented any supply of moisture from entering the area from its source region to the south. This lack of precipitation and cloudiness gave excellent conditions for warming in the interior and was associated with a well-developed sea breeze along the coastal regions of California. The existence of the sea breeze can best be seen from the wind rose at Los Angeles (Chart I). Its effect on the temperature anomaly (Chart I) as well as the percentage of clear skies (Chart IV) is quite pronounced along the coast. These three features go together with this type of regime, especially in the spring, when the water temperatures are much colder than the land during the day.

Excessive amounts of precipitation fell during the month in North Dakota and northern Minnesota, accompanying the mean trough and the center of negative 700-mb. height anomaly. This anomalous precipitation caused flood conditions over much of the region, the most publicized of which was the near disaster in Winnepeg which is located on the northward flowing Red River. Aggravating this flood condition was the melting of a snow cover which existed over much of the Red River watershed at the beginning of the month. Other less severe flood conditions occurred during the month in Arkansas and Oklahoma. The excessive precipitation in this region, mainly in the form of showers, was also associated with the trough in the southwestern United States. The stronger-than-normal southerly flow, both at sea level and aloft, transported considerable amounts of moisture from its source region in the Gulf of Mexico. Another related fact was the existence of strong cyclonic curvature of the sea-level isobars in the area (Chart VI). The precipitation spread eastward from Oklahoma with the flow aloft, along an east-west minimum in the sea-level pressure anomalies. The minimum was reflected in the sea-level isobars by the cyclonic curvature in the region of Tennessee. The deficient precipitation extending from northwestern Indiana along the northern border to Maine lay between the main cyclone track, well to the north, and the belt of showery precipitation to the south. Not a single cyclone entered this region during the month. A maximum in the sea-level pressure anomaly over this area was reflected in the sea-level isobars by predominant anticyclonic curvature. A stronger-than-normal ridge aloft also covers much of this region.

The below-normal surface temperatures centered in Wyoming (Chart I) gave way to above-normal temperatures to the east of the 700-mb. mean trough. Here the 700-mb. contours had only a slight component from the south, but the field of 700-mb. height anomaly shows that this flow had a stronger southerly component than normal. The above-normal temperatures in the eastern United States were also related to the above-normal 700-mb. heights. The belt of maximum above-normal temperatures was found in the region where the sum of the contributions from the above-normal heights and the stronger-than-normal southerly flow was greatest. This is mainly to the west of the maximum of positive height anomalies of the 700-mb. surface.

The existence of below-normal surface temperatures along the middle Atlantic coast of the United States might at first seem puzzling since it occurred very close to the region of maximum 700-mb. height anomaly. It is well known, however, that the weather of coastal regions is greatly influenced and modified by the adjacent oceans, especially in the spring when the ocean temperature lags that of the land. The easterly and northeasterly flows

indicated by the anomalies of the sea level pressure and 700-mb. height show that the air trajectories in this region were more predominantly maritime than normal. The frequent passage of anticyclones (Chart II) north of this region also is indicative of the frequency of easterly flow in this area. The association between persistent stratus conditions and the predominantly easterly regime of the type which occurred during this month is well known. The percentage of clear skies during the daytime as given in chart IV shows the deficiency of sunshine in this area. The region off the east coast between 35° and 40° N. was a frequent seat of cyclonic development (Chart III). The northeasterly flow relative to normal along and off the coast and the proximity of the polar anticyclone tracks were associated with the juxtaposition of cool polar maritime air and the warmer air over the Gulf Stream. A solenoidal field favorable to cyclonic development was established. These cyclones moved across the Atlantic mainly along the east-west sea level trough and the mean flow aloft. The main storm track across the Atlantic was well to the south of normal due to the predominance of blocking conditions in the north Atlantic during the month (see fig. 1). As can be seen from the cyclone tracks (Chart III) the Lows were blocked completely from moving into the northeast Atlantic and some storms were even forced to recurve toward the west.

It is interesting to note that over many portions of the United States and adjacent oceans, the weather and circulation for May was a complete reversal from that of the preceding month (see fig. 1 of the article by Winston and Charts I and IV in the April 1950, Monthly Weather Review). In April the eastern half of the United States at the 700-mb. level was under the influence of a mean trough, cyclonic curvature, and below-normal heights, while the western half of the United States was under the influence of a mean ridge. The contrast in circulation patterns for the two months caused equally contrasting surface temperature and precipitation anomalies over the United States.

893180—50——2

# SOME SYNOPTIC ASPECTS OF THE HOT WEATHER IN CALIFORNIA, MAY 29–31, 1950

DONNELL H. GOULD AND LEWIS C. NORTON

WBAN Analysis Center, U. S. Weather Bureau

Washington, D. C.

During the last 3 days of May 1950, temperatures in the inland sections of California rose to near record levels for the season. At most reporting stations the highest was reached on May 30 though some points in the southern portion of the State reported higher temperatures on the 31st. Figure 1 shows the maximum temperatures on each of the last 3 days of the month together with the 24-hour change in maximum temperature for each day. The highs of 108° F. at Red Bluff, 106° at Bakersfield, and 100° at Sacramento compare with absolute maxima for May of 110°, 110°, and 103°, respectively.

Hot weather extended to the coast only at San Francisco, where the highest temperature was 92°, reached on May 29. Although this is 5° below the May record of 97°, it is far above the average maximum temperature of 63°. The sectional weather charts in figure 2 show the westward extent of the warm air at 1030 PST, and 1130 PST, May 29, when the temperature at San Francisco rose from 79° at 1030 PST to 91° at 1130 PST. By 1530 PST (chart not shown), the temperature had dropped to 84°. On May 30 the cool sea breeze advanced almost to Sacramento and temperatures in the San Francisco Bay area dropped to near normal levels (fig. 1).

The following paragraphs present some of the synoptic aspects leading to the establishment and breakdown of this high temperature situation of May 29–31, 1950.

At 0030 GMT, May 28 (chart not shown), a rapidly deepening Low in the North Pacific had moved northeastward to a position near 49°N, 153°W. As this Low deepened and extended to higher levels in the atmosphere, winds aloft in the area south and east of the Low backed to southwesterly and increased in speed. On the 500-mb. chart for 0300 GMT, May 28 (fig. 3) this area of strong southwesterly winds aloft is shown as a broad band ex-

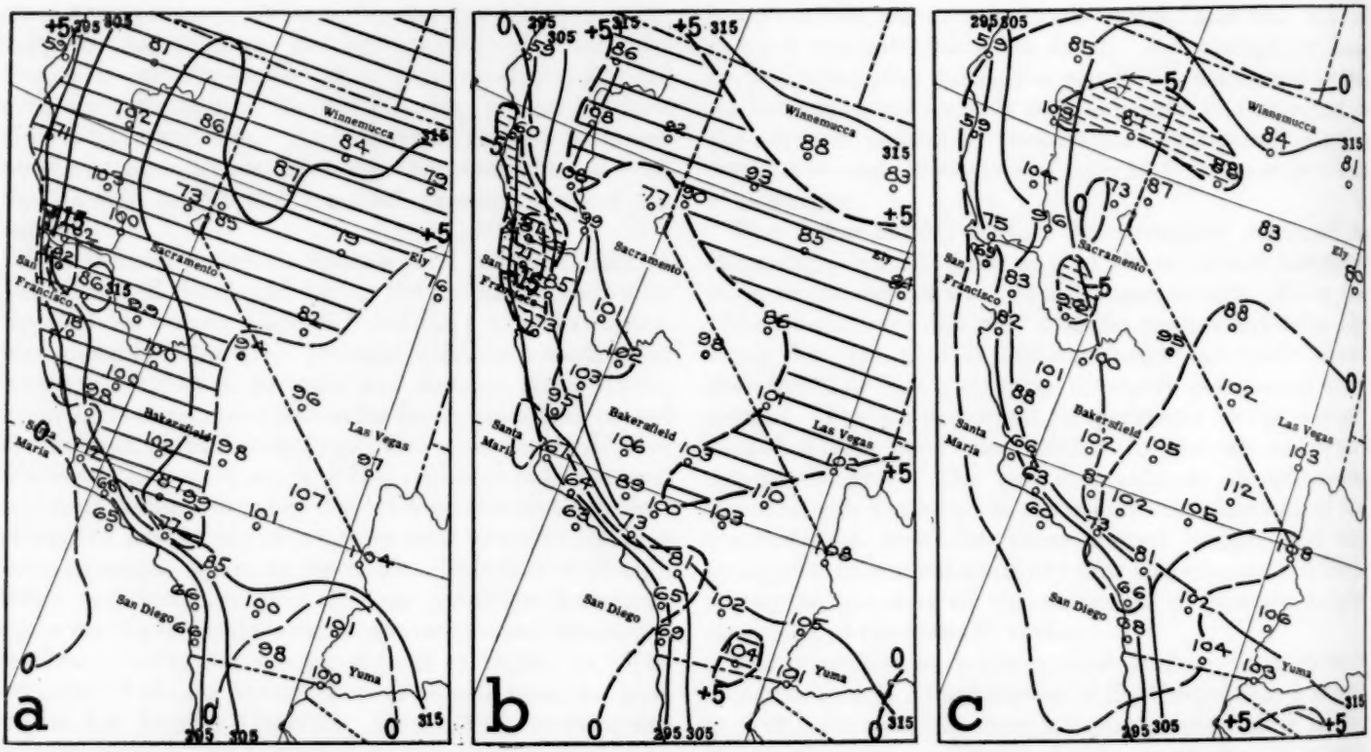


FIGURE 1.—Maximum potential temperature charts for (a) May 29, (b) May 30, and (c) May 31, 1950. Solid lines are isotherms of the potential temperature (in degrees absolute) of reported maxima. Broken lines show 24-hour change in maximum temperature (in degrees Fahrenheit). Solid hatching covers areas of 5° F. or more of 24-hour warming and broken hatching areas of 5° or more of 24-hour cooling. Actual reported maximum temperatures (in degrees Fahrenheit) are shown at individual stations.

tending approximately from 160°W to 145°W, and between latitudes 40° N and 50° N. Contour gradients indicate that wind speeds in this area were 80 to 100 knots.

East of the area of strong southwesterlies at 500 mb. (fig. 3) there was a marked north-south temperature gradient north of latitude 45° N. The accompanying warm advection in the current approaching the coast from northern California to British Columbia indicated rising contour heights in the vicinity of the Washington and British Columbia coastal area. Also, as shown in figure 3, a west-northwest wind of about 50 knots in southwestern Oregon was moving toward an area of appreciably weaker gradient in northern Nevada. This movement into weaker gradient required supergradient flow over northern Nevada (assuming eastward movement of the contour system to be less than the wind speed), and consequently a change to more anticyclonic curvature. The result was a shifting of winds over Nevada to more northerly. To the west of southern Oregon, over the Pacific, the contour gradient (fig. 3) indicated that winds of 50 knots or better should have continued to be fed into southwestern Oregon until there was an appreciable change in the contour pattern. Assuming this condition to hold through a reasonably deep layer of the atmosphere, any continued anticyclonic turning of successive streamlines from southwestern Oregon through Nevada should have tended to carry mass across the contours and eventually to produce a contour gradient more nearly corresponding to the flow.

To the southward, a similar condition of strong winds flowing into an area of weaker gradient is indicated on figure 3 where winds 300 or 400 miles west-northwest of the northern California coast are moving into the weaker

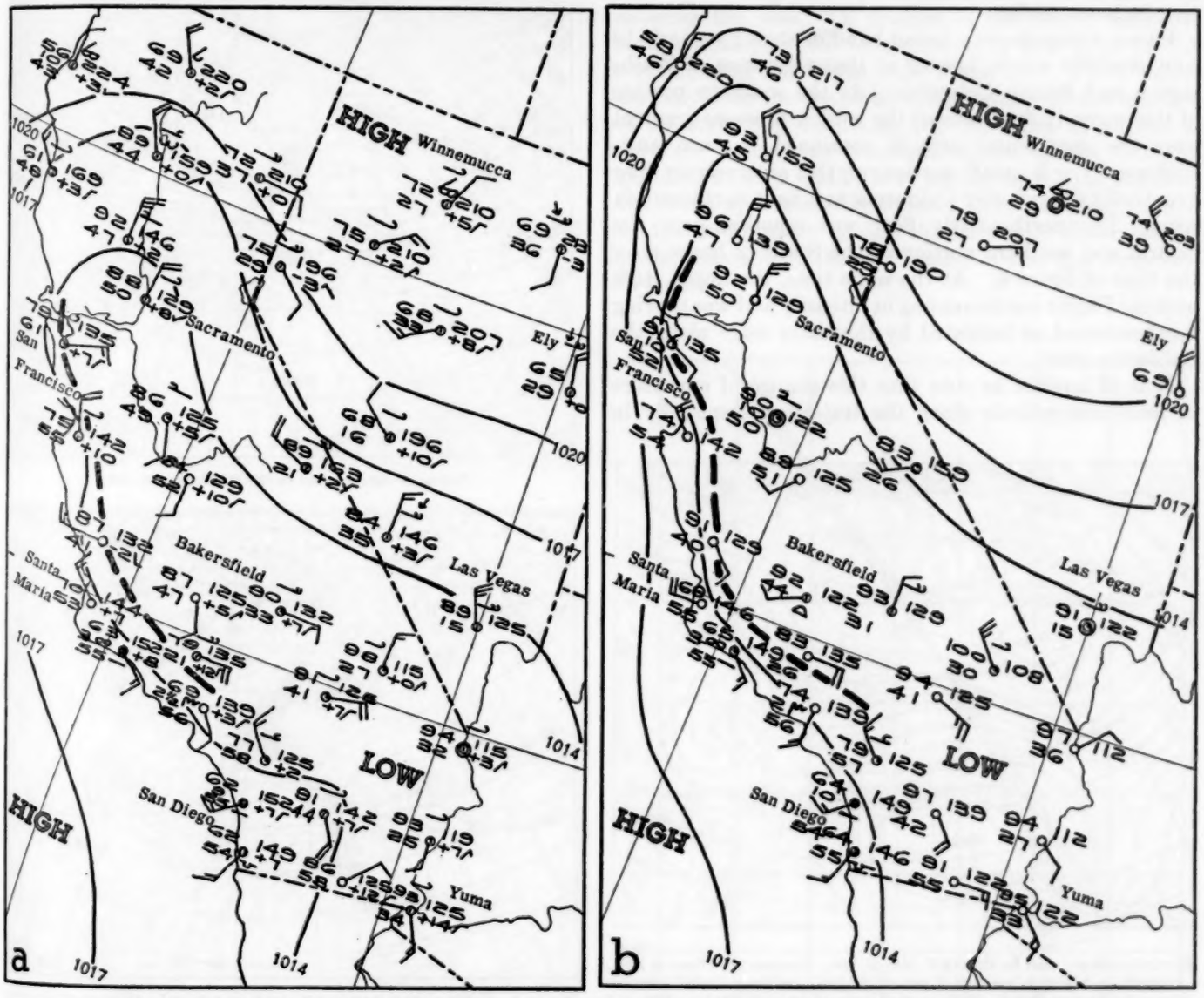


FIGURE 2.—Sectional surface weather charts for (a) 1030 PST and (b) 1130 PST, May 29, 1950. Heavy dashed line shows western boundary of warm air.

gradient over northern California. Existence of the stronger winds was less certain than over southwestern Oregon, but seems to be required by any reasonable interpretation of all available data. Thus conditions were favorable for winds over both California and Nevada to become more northerly during the ensuing 12 hours, as was verified by reports of generally northwest winds for 500 mb. at 1500 GMT, on the 28th (chart not shown). The shifting of direction continued, and at 0300 GMT on the 29th (fig. 4), 500-mb. winds over both States were almost straight northerly. Heights had risen at Tatoosh Island, Wash., and fallen slightly at Ely and Las Vegas, Nev. It should be noted that the northerly winds over California and Nevada were entirely in the warm air and that the strong north-south temperature gradient (in a band extending generally westward from Central British Columbia on fig. 4) was even farther north than its position 24 hours earlier.

Figure 4 also shows a broad band of strong westerly to southwesterly winds, located at that time west of Washington and British Columbia. As the southern portion of this westerly flow entered the weaker pressure gradient over the continental area it continued to turn anticyclonically. A small portion of the anticyclonic flow eventually arrived over California as a light northeasterly wind. The northeasterly flow was reported over the central and southern portion of the State 12 hours after the time of figure 4. At the same time, the upper High over the Pacific was increasing in intensity and was moving northeastward as indicated by the sharp ridge along the California coast.

It is of interest to note that this change of curvature to more anticyclonic along the trajectory (especially in the northerly current) indicates horizontal divergence, by the principal of conservation of vorticity. There was a similar change of curvature at levels below 500 mb. (not illustrated). Appreciable divergence in the lower levels was necessarily accompanied by subsidence, an important factor in producing high surface temperature when combined with strong insolation at the ground. Some further subsidence at lower levels took place in air which reached the Great Valley of California, because of downslope motion on the lee side of high mountain ranges.

The surface weather chart for 0030 GMT, May 29 (fig. 5) shows a deep Low located off the coast of Southeast Alaska and a cold occlusion just entering British Columbia. Subsequently this front moved rapidly eastward in accordance with strong westerly flow aloft. There was, however, little southward movement of the cold air;

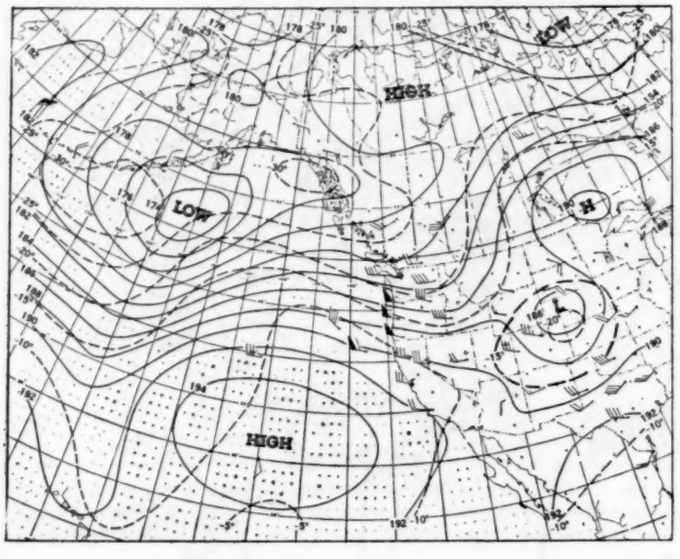


FIGURE 3.—500-mb. chart for 0300 GMT, May 28, 1950. Contours (solid lines) at 200-ft. intervals are labeled in hundreds of geopotential feet. Isotherms (dashed lines) are drawn for intervals of 5° C. Barbs on wind shafts are for wind speeds in knots (full barb for every 10 knots, half barb for every 5 knots and pennant for every 50 knots).

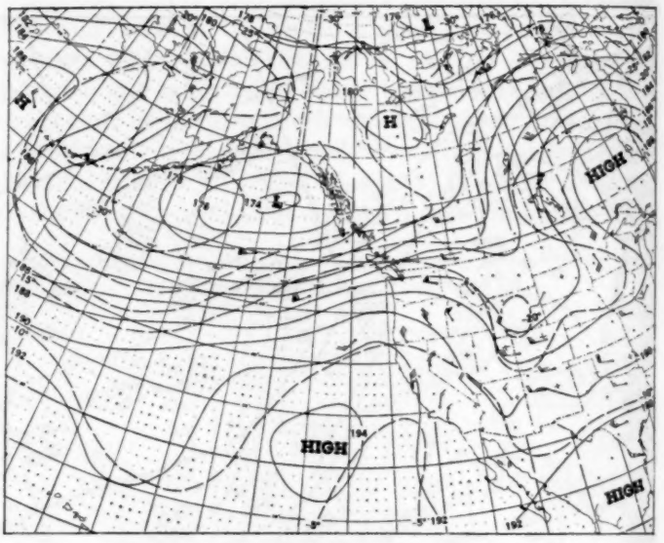


FIGURE 4.—500-mb. chart for 0300 GMT, May 29, 1950.

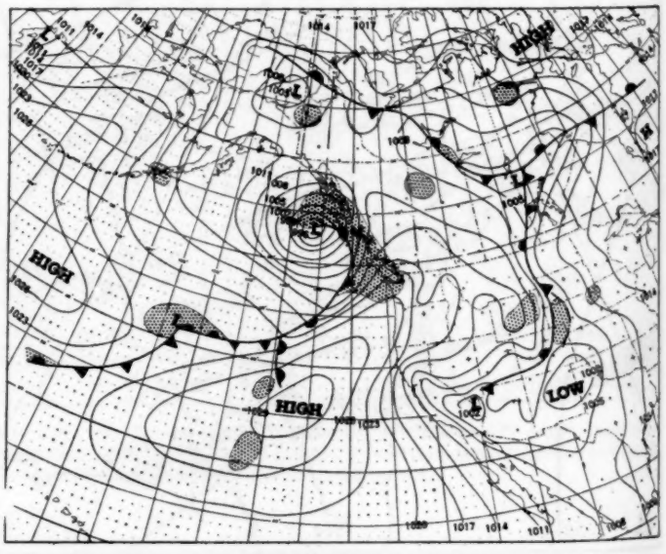


FIGURE 5.—Surface weather chart for 0030 GMT, May 29, 1950. Shading indicates areas of active precipitation.

the portion of the cold front which later trailed westward became stationary and by 0030 GMT May 31 (chart not shown) had frontolyzed over the mountains of extreme northern California.

As the deep Low off Southeast Alaska (fig. 5) filled and moved northward, pressures rose rapidly in the Washington and British Columbia area and the ridge continued to intensify aloft. By 0030 GMT, May 30 (fig. 6) a High center of 1030 mb. was located off the Washington coast and a ridge extended southeastward through Washington and Oregon into Nevada, producing an easterly flow downslope into California from Nevada where potential temperatures were already quite high (fig. 1a).

Optimum conditions for hot weather in California were reached on May 29 and 30. At upper levels the Pacific High had increased in intensity at all levels and moved to the northeast. Maximum northeastward displacement of the High at 500 mb. was reached at 1500 GMT May 30 (fig. 7) when it was centered just off the central California coast with a strong ridge extending northward into Southeast Alaska. Winds at this level over California from Sacramento southward had an easterly component. The easterly flow was even more pronounced at levels below 500 mb., a condition favorable for very high temperatures in the interior valleys of California.

Accompanying the increased strength of the High was a slow but continuous warming at most levels below 500 mb. throughout the California-Nevada area. In figures 8, 9, and 10 this warming is shown by soundings at 24-hour intervals over Oakland, Calif., and Ely and Las Vegas, Nev. Above the surface inversion the soundings are very similar, showing the homogeniety of the air mass covering the area. Of interest is the nearly adiabatic lapse rate at potential temperatures of 314° A to 318° A over Ely and Las Vegas (figs. 9 and 10). These values are very near the potential temperatures of the maxima at the surface in California (fig. 1). Also of interest is the very strong, low inversion shown on the Oakland sounding at 0300 GMT, May 30 (fig. 8). This sounding was taken approximately 8 hours after the occurrence of the maximum of 92° at San Francisco and illustrates the reestablishment of the sea breeze in the San Francisco Bay area.

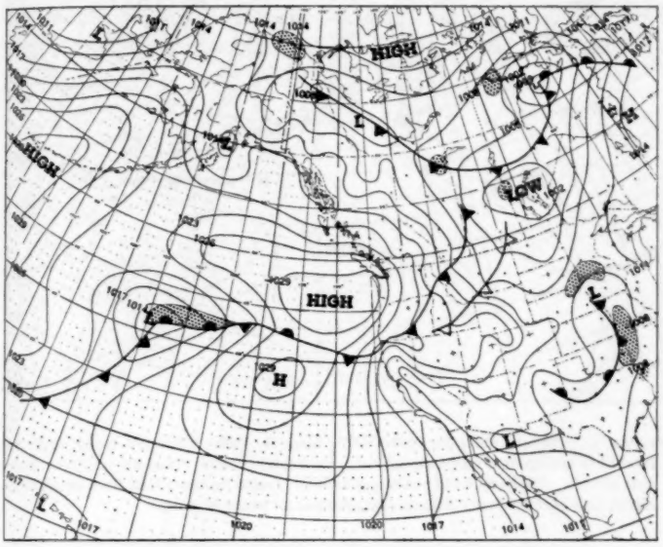


FIGURE 6.—Surface weather chart for 0030 GMT, May 30, 1950. Shading indicates areas of active precipitation.

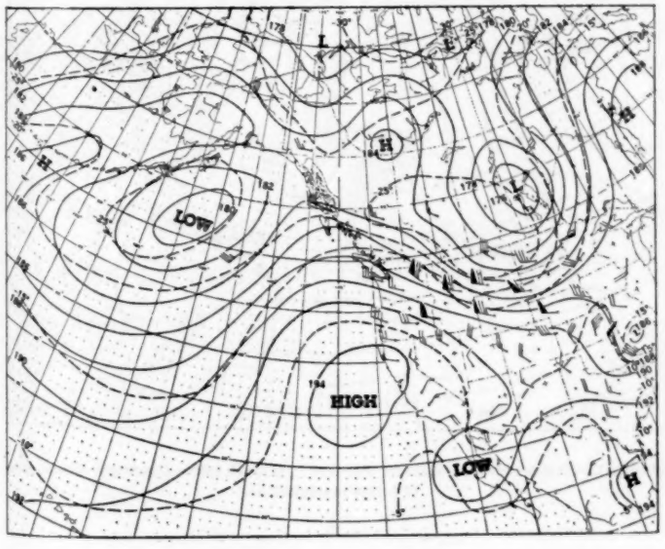


Figure 7.—500-mb. chart for 1500 GMT, May 30, 1950.

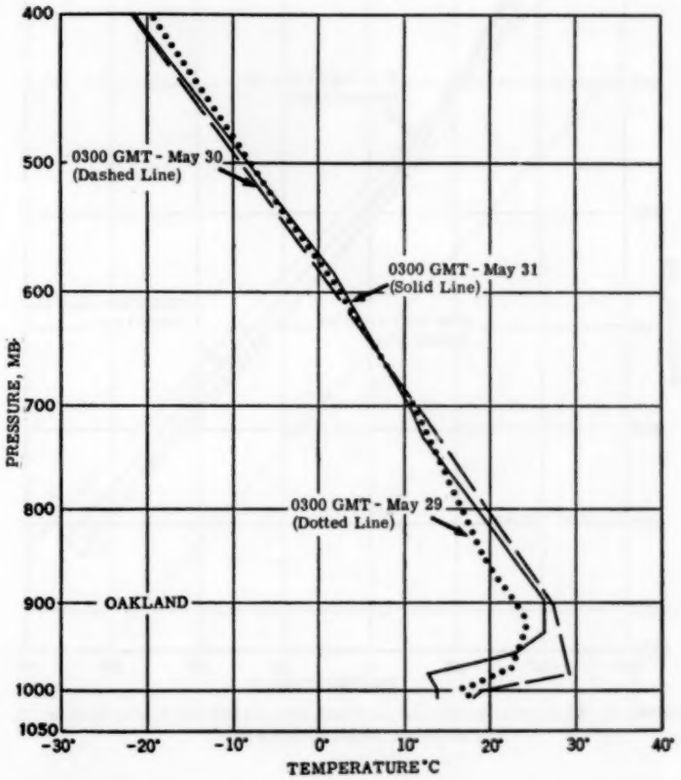


FIGURE 8.—Upper air soundings over Oakland, Calif., for 0300 GMT, May 29, 30, and 31, 1950, plotted on pseudo-adiabatic chart.

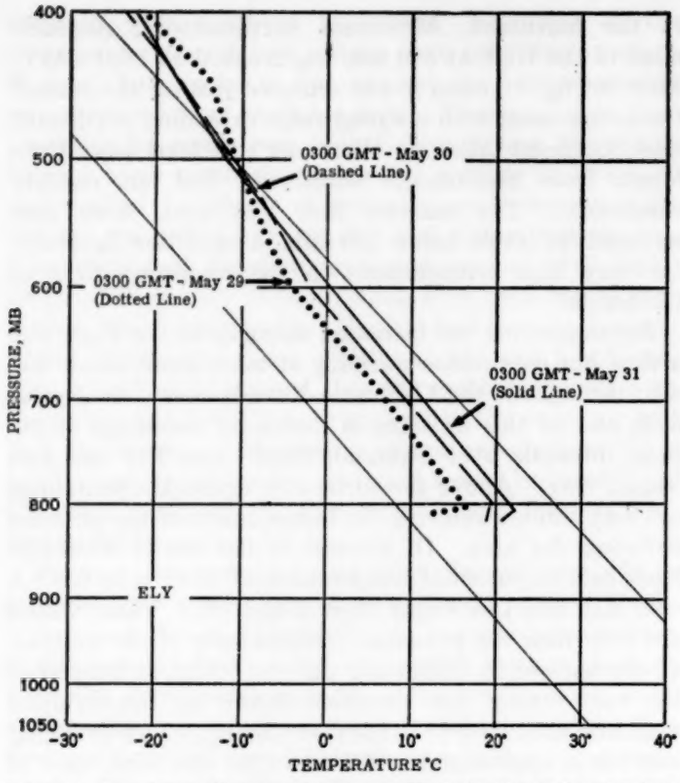


FIGURE 9.—Upper air soundings over Ely, Nev., for 0300 GMT, May 29, 30, and 31, 1950, plotted on pseudo-adiabatic chart.

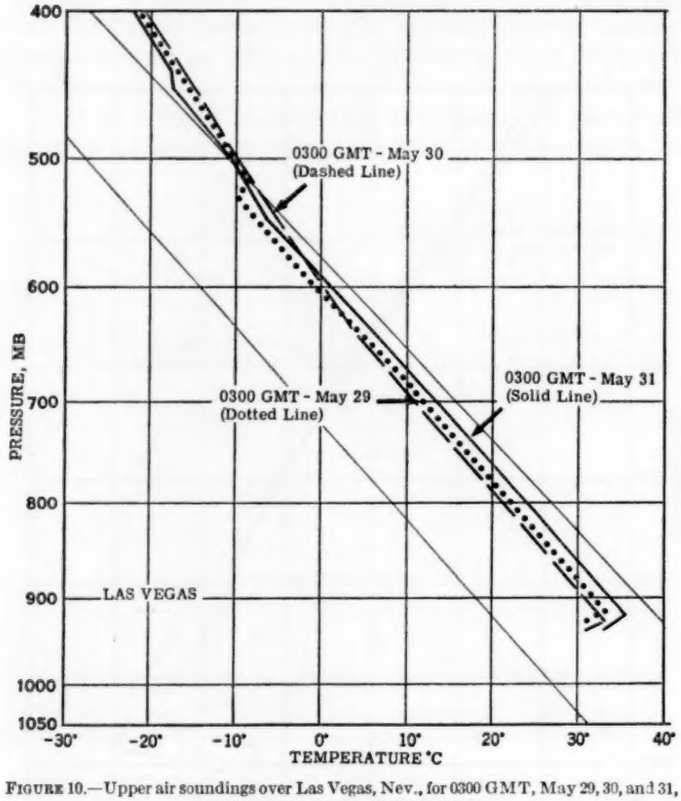


FIGURE 10.—Upper air soundings over Las Vegas, Nev., for 0300 GMT, May 29, 30, and 31, 1950 plotted on pseudo-adiabatic chart.

Maximum temperatures at the 700-mb. level were reached at 0300 GMT, May 31 (fig. 11). Temperatures between 11° C and 12° C were far above normal [1] and approached the absolute maxima [2] for that level at Ely and Oakland. The isotherms in figure 11 show temperatures to be much higher over the continent than in the portion of the High over the ocean to the west. They were also higher than any which could have resulted from horizontal advection and as previously mentioned, were evidently caused by the combined effect of strong surface heating over land and subsidence in the eastern portion of the Pacific High cell.

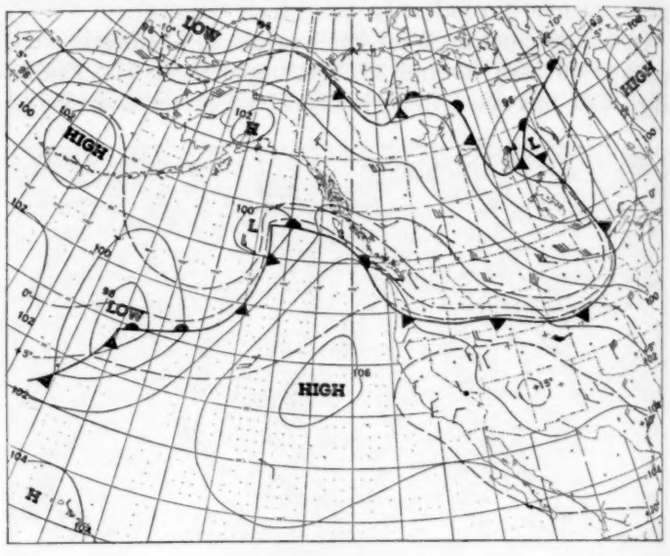


FIGURE 11.—700-mb. chart for 0300 GMT, May 31, 1950. Contours (solid lines) are labeled in hundreds of geopotential feet. Isotherms (dashed lines) are drawn for intervals of 5° C. Barbs on wind shafts are for wind speeds in knots (full barb for every 10 knots, half barb for every 5 knots and pennant for every 50 knots).

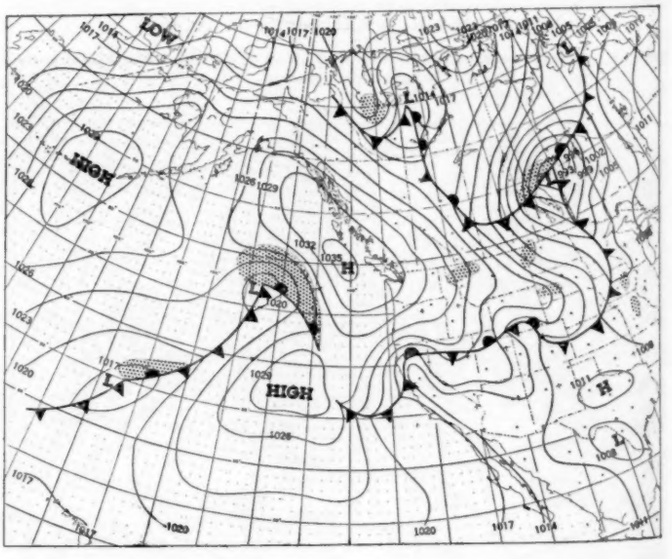


FIGURE 12.—Surface weather chart for 1830 GMT, May 30, 1950. Shading indicates areas of active precipitation.

Coincident with the building of the warm High aloft the surface High continued to increase in intensity off the Washington-British Columbia coast reaching a maximum at the center of 1036 mb. just south of Cape St. James, B. C., at 1830 GMT, May 30 (fig. 12). A pronounced ridge continued to extend southeastward into Nevada. The pressure of 1036 mb. near Cape St. James was within about 1 millibar of the highest ever recorded at that location during May.

Although figure 12 represents conditions near the time of peak temperatures in California, it also shows some indication of the breakdown of these conditions. The Low at 47° N, 143° W, while not deep, was too well marked to disappear quickly. It subsequently filled slowly, but as it approached the coast there was a rapid breakdown of the High.

By 1500 GMT, May 31 (chart not shown), the eastern and northern extension of the High at upper levels had almost entirely disappeared, and cooler air was moving into northern California and Nevada. This flow was generally westerly at 500 mb. and northwesterly at the 700-mb. level. The maximum potential temperature chart (fig. 1) shows appreciable cooling in northern California on May 31 though many interior valley stations still reported temperatures of 100° or more. Further cooling was more gradual but by June 2 (chart not shown) the heat had moderated in all but the extreme southeast section of the State.

## REFERENCES

1. U. S. Weather Bureau, "Upper Air Average Values of Temperature, Pressure, and Relative Humidity over the United States and Alaska," Washington, D. C., May 1945 (reprinted as *Technical Paper No. 6*, April 1949).
2. U. S. Weather Bureau, "Extreme Temperatures in the Upper Air," *Technical Paper No. 3*, Washington, D. C., July 1947.

U. S. GOVERNMENT PRINTING OFFICE: 1950

Chart I. Departure (°F.) of the Mean Temperature from the Normal, and Wind Roses for Selected Stations, May 1950

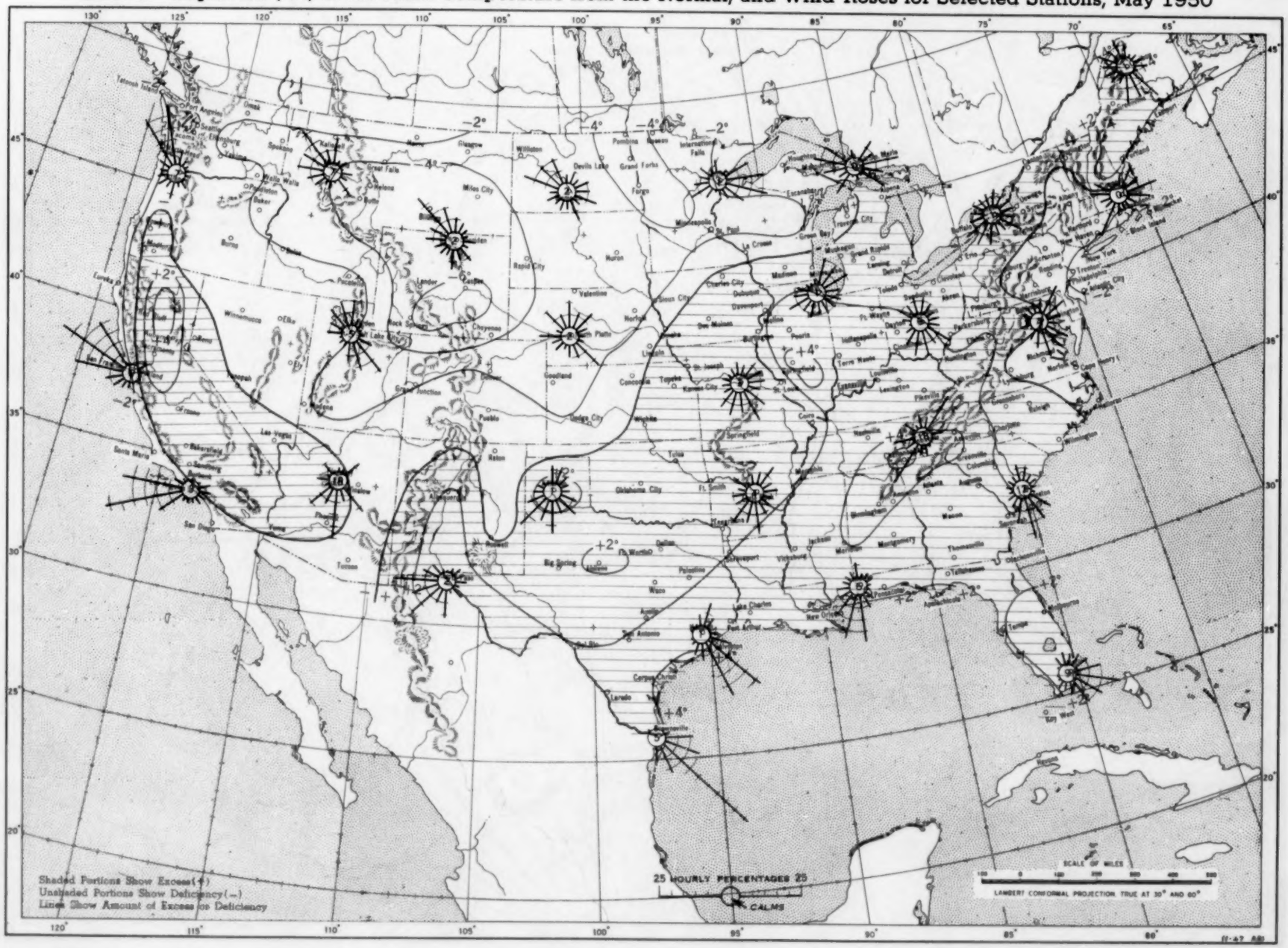

**Chart II. Tracks of Centers of Anticyclones, May 1950.** **(Inset) Departure of Monthly Mean Pressure from Normal**

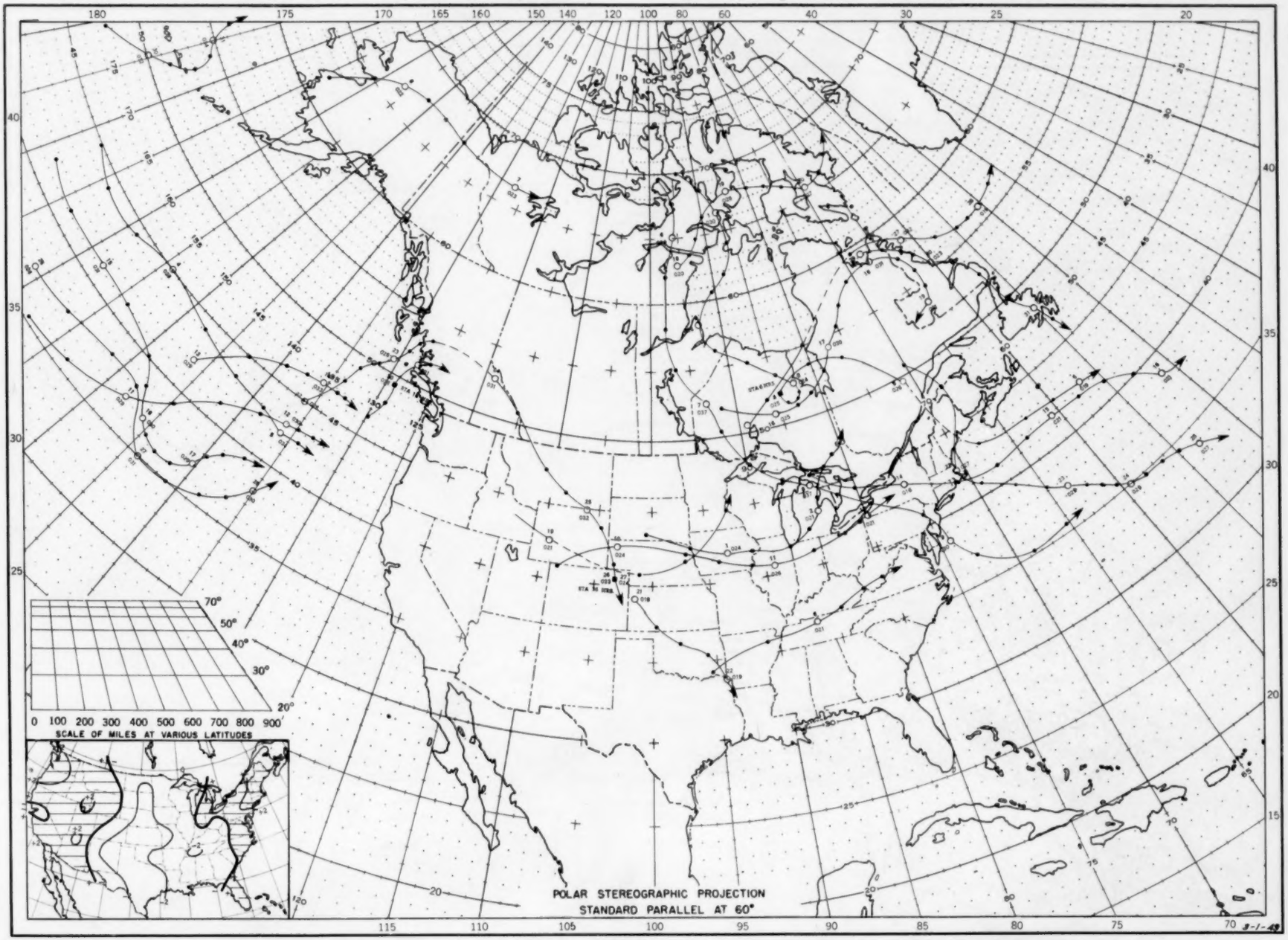


Circle indicates position of anticyclone at 7:30 a. m. (75th meridian time). Dots indicate intervening 6-hourly positions. Figure above circle indicates date, and figure below, pressure to nearest millibar. Only those centers which could be identified for 24 hours or more are included.

**Chart III. Tracks of Centers of Cyclones, May 1950.** **(Inset) Change in Mean Pressure from Preceding Month**


Circle indicates position of cyclone at 7:30 a. m. (75th meridian time) Dots indicate intervening 6-hourly positions. Figure above circle indicates date, and figure below, pressure to nearest millibar. Only those centers which could be identified for 24 hours or more are included.

## Chart IV. Percentage of Clear Sky Between Sunrise and Sunset, May 1950

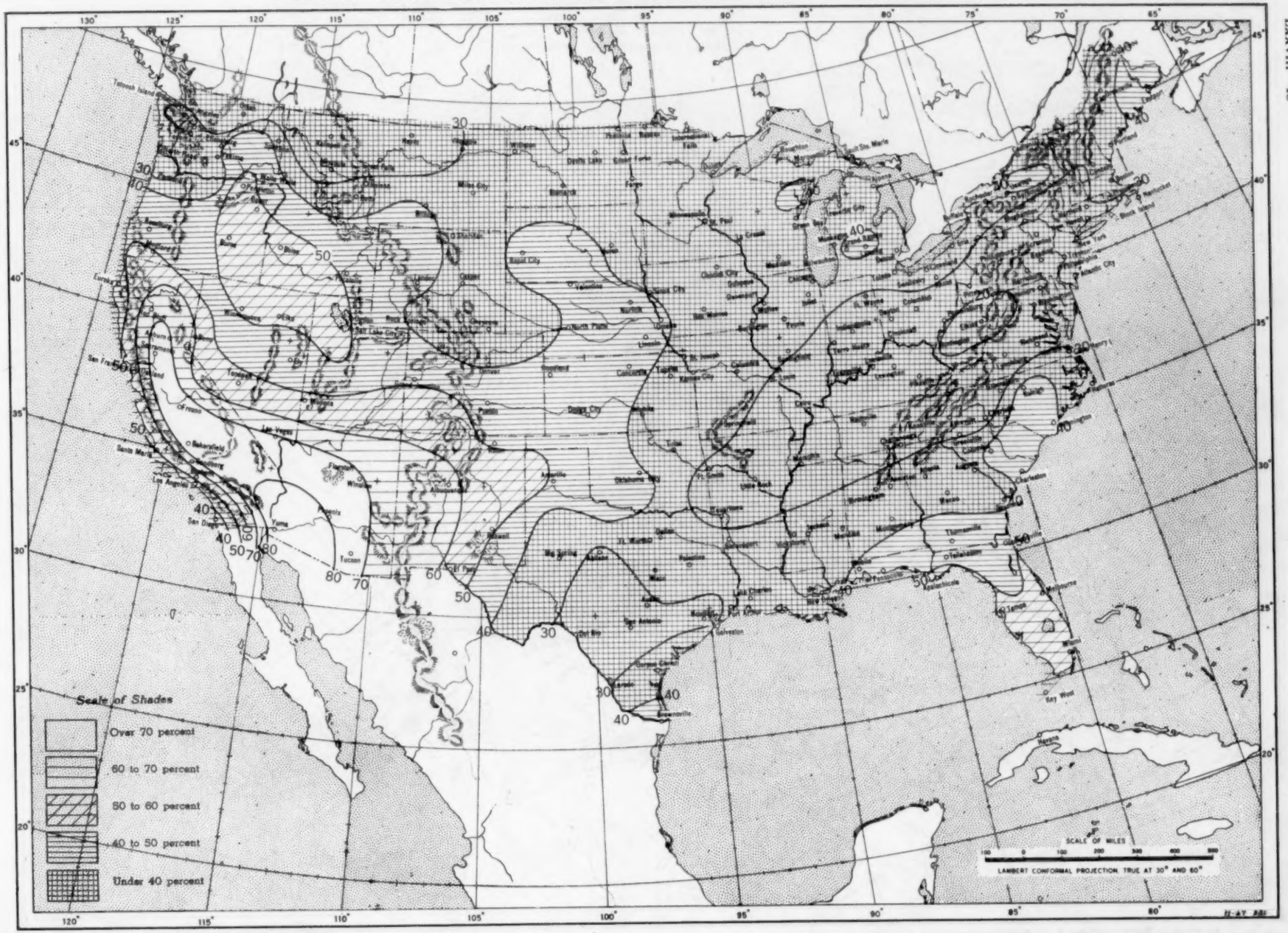

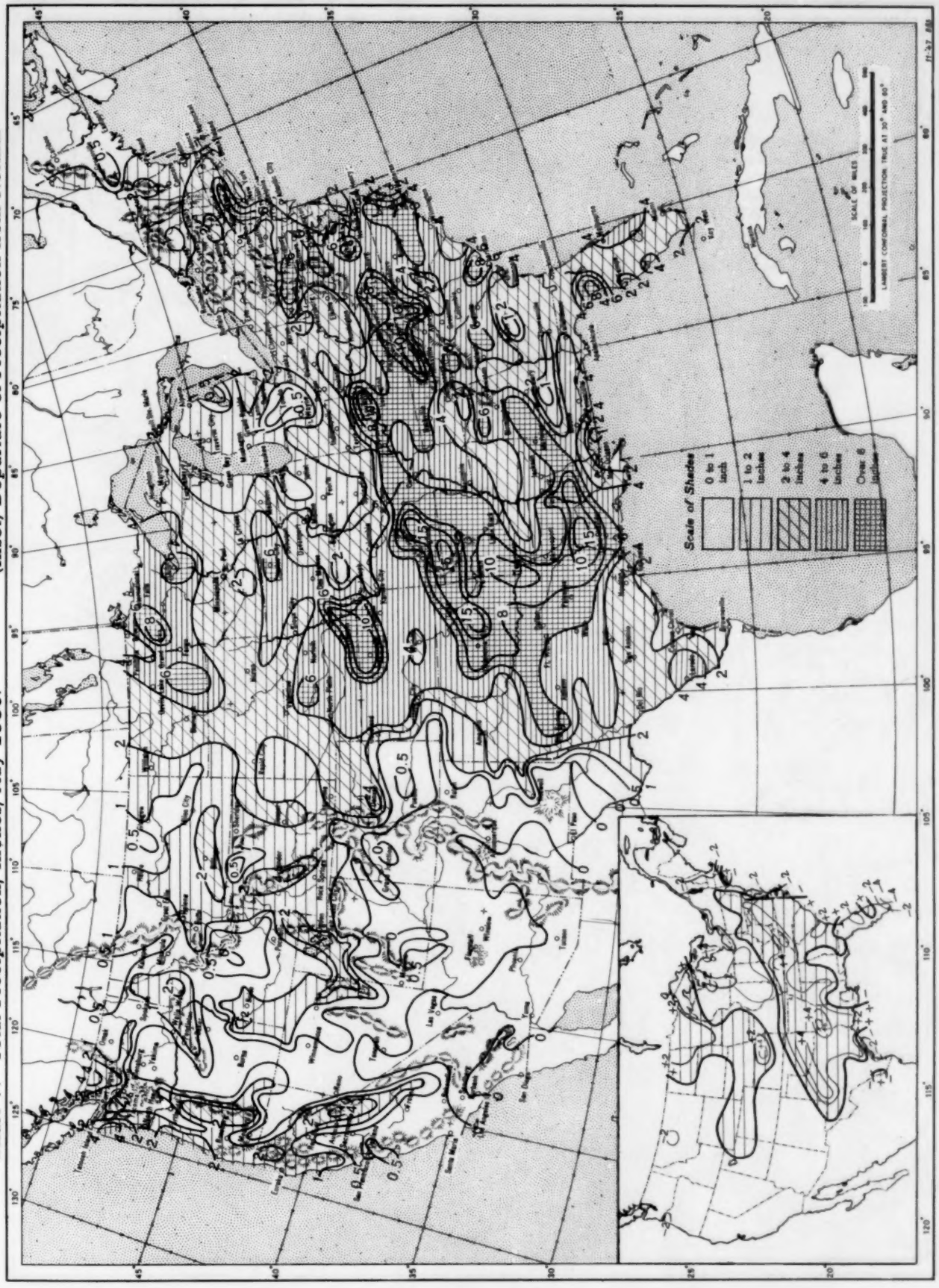


Chart V. Total Precipitation, Inches, May 1950. (Inset) Departure of Precipitation from Normal

## Chart VI. Mean Isobars (mb.) at Sea Level and Mean Isotherms (°F.) at Surface., May 1950

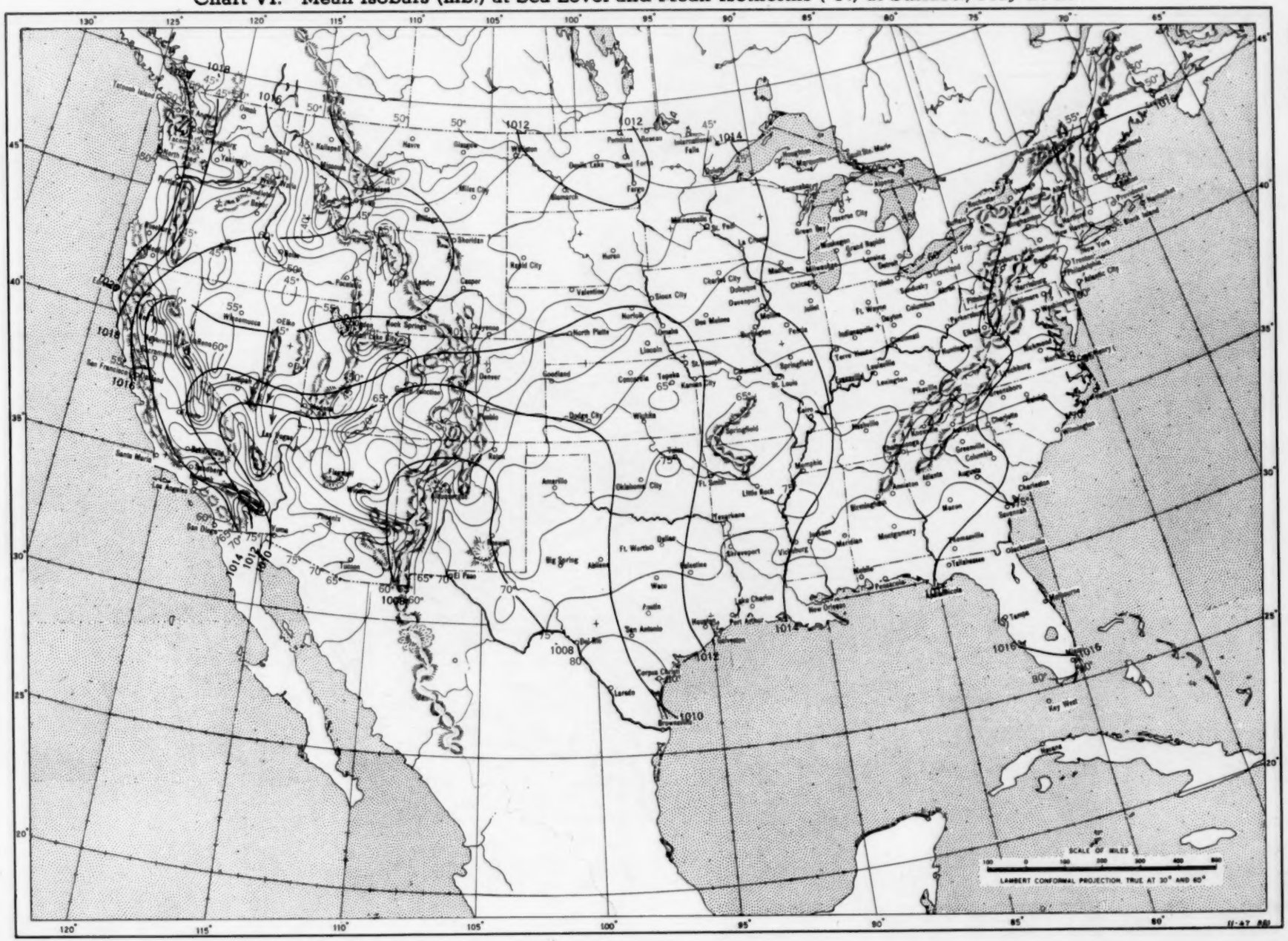

Chart VIII, May 1950. Contour Lines of Mean Dynamic Height (Geopotential) in Units of 0.98 Dynamic Meters and Mean Isotherms in Degrees Centigrade for the 850-millibar Pressure Surface, and Resultant Winds at 1,500 Meters (m. s. l.)

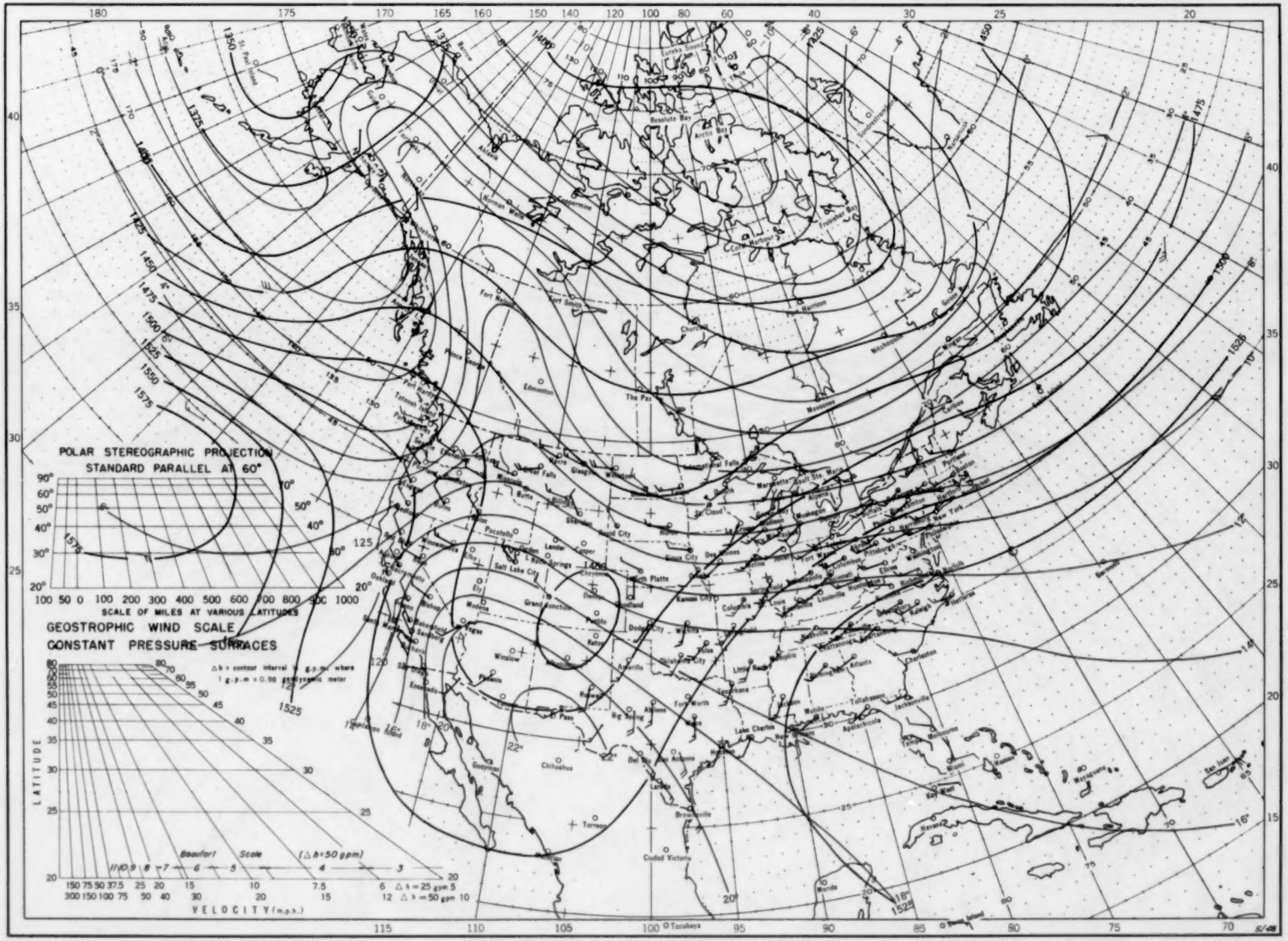


Contour lines and isotherms based on radiosonde observations at 0300 G. C. T. Winds indicated by black arrows based on pilot balloon observations at 2100 G. C. T.; those indicated by red arrows based on rawins taken at 0300 G. C. T.

Chart IX, May 1950. Contour Lines of Mean Dynamic Height (Geopotential) in Units of 0.98 Dynamic Meters and Mean Isotherms in Degrees Centigrade for the 700-millibar Pressure Surface, and Resultant Winds at 3,000 Meters (m. s. l.)

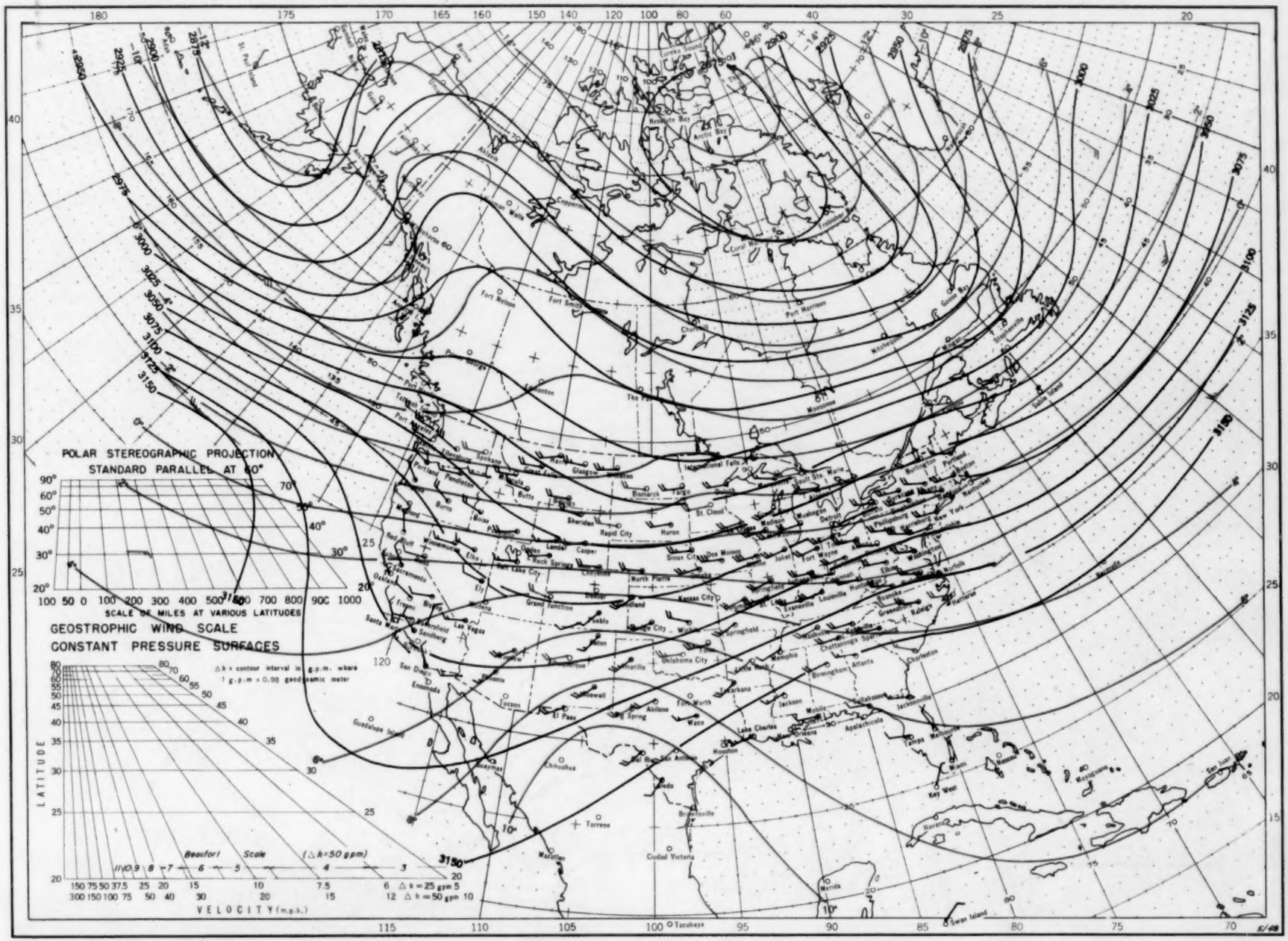


Contour lines and isotherms based on radiosonde observations at 0300 G. C. T. Winds indicated by black arrows based on pilot balloon observations at 2100 G. C. T.; those indicated by red arrows based on rawins taken at 0300 G. C. T.

Chart X, May 1950. Contour Lines of Mean Dynamic Height (Geopotential) in Units of 0.98 Dynamic Meters and Mean Isotherms in Degrees Centigrade for the 500-millibar Pressure Surface, and Resultant Winds at 5,000 Meters (m. s. l.)

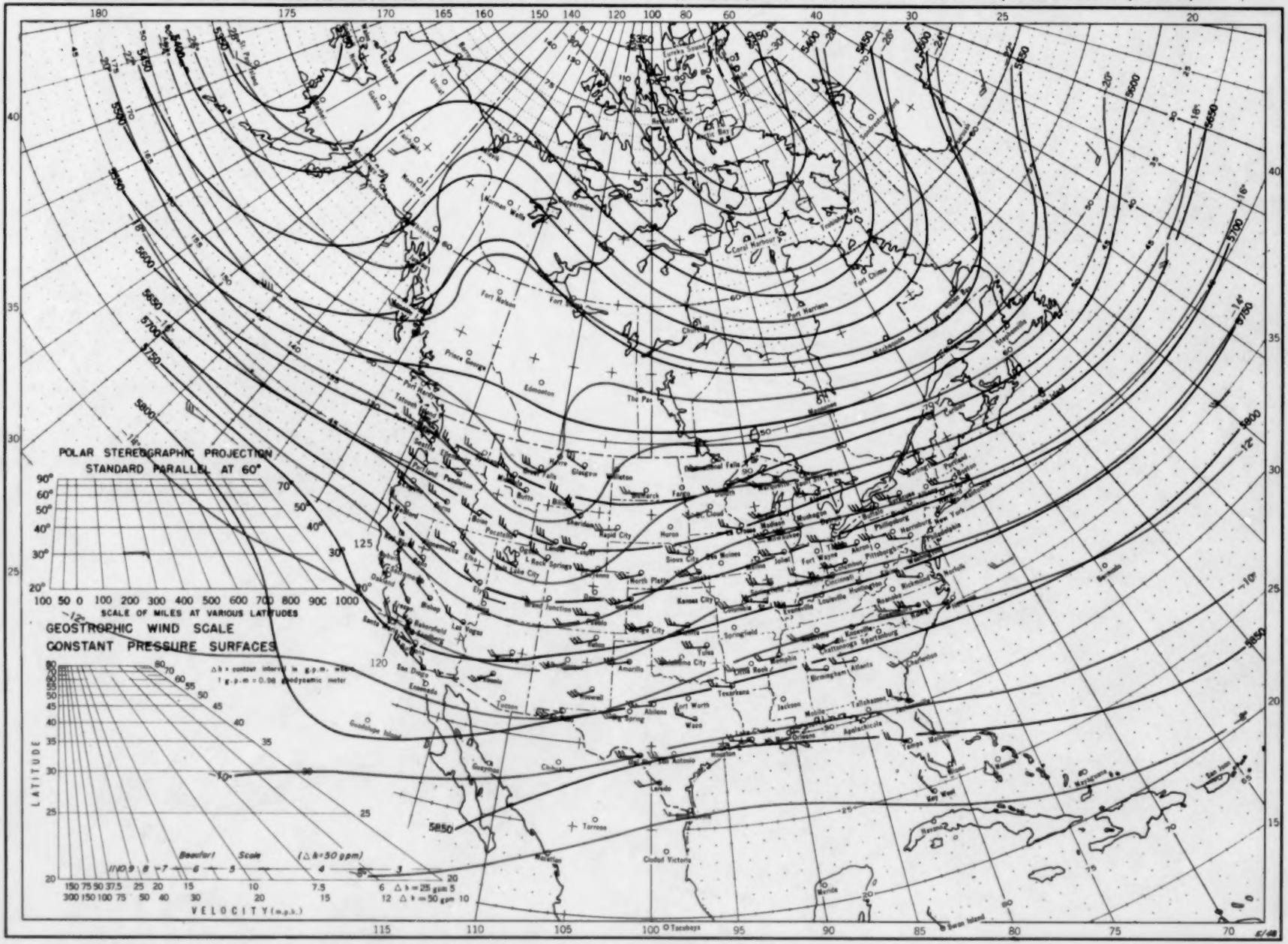


Contour lines and isotherms based on radiosonde observations at 0300 G. C. T. Winds indicated by black arrows based on pilot balloon observations at 2100 G. C. T.; those indicated by red arrows based on rawins taken at 0300 G. C. T.

Chart XI, May 1950. Contour Lines of Mean Dynamic Height (Geopotential) in Units of 0.98 Dynamic Meters and Mean Isotherms in Degrees Centigrade for the 300-millibar Pressure Surface, and Resultant Winds at 10,000 Meters (m. s. l.)

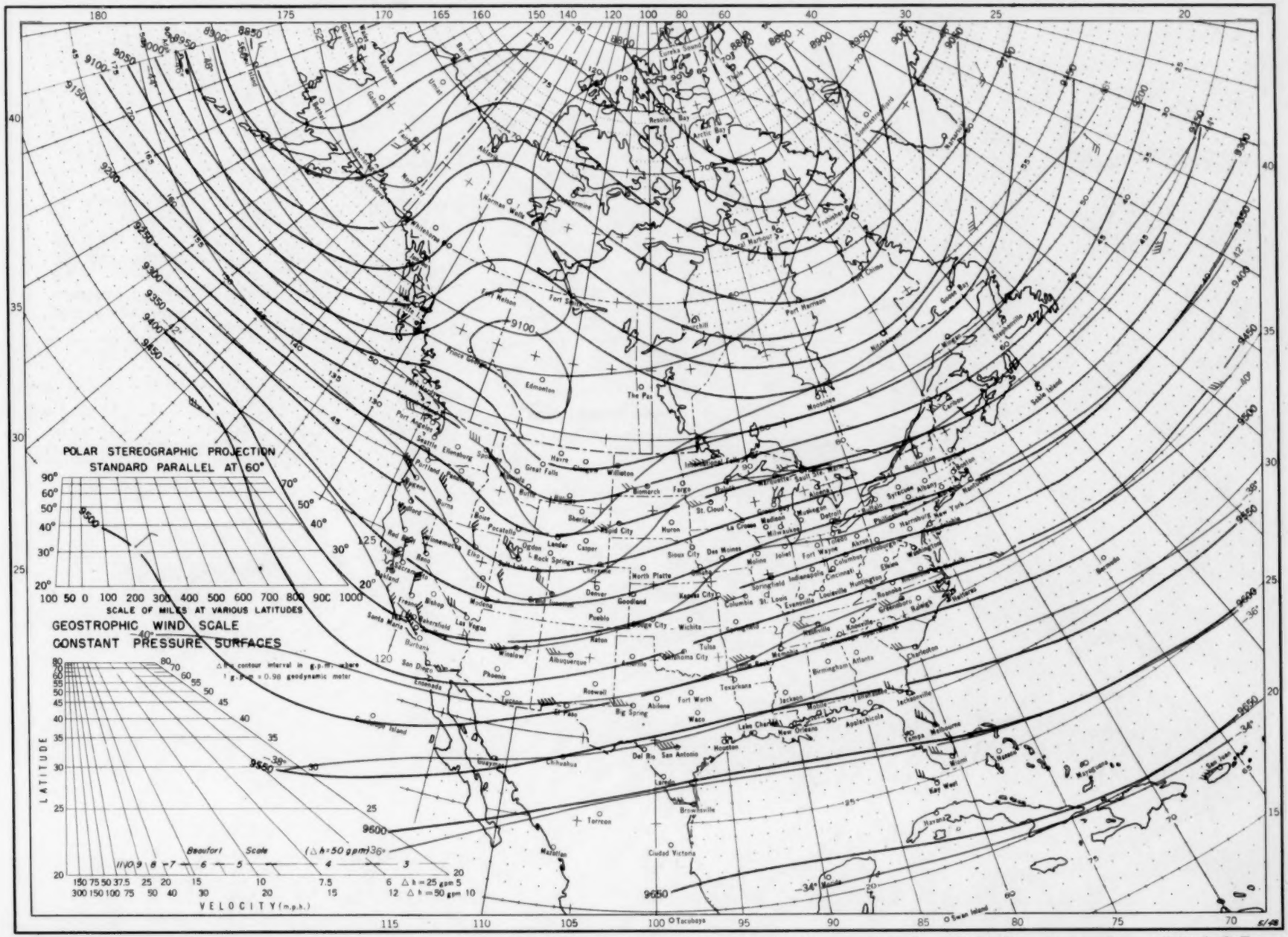


Contour lines and isotherms based on radiosonde observations at 0300 G. C. T. Winds indicated by black arrows based on pilot balloon observations at 2100 G. C. T.; those indicated by red arrows based on rawins taken at 0300 G. C. T.